Phase diagram of the asymmetric Hubbard model

Pavol Farkašovský
Institute of Experimental Physics, Slovak Academy of Sciences, Watsonova 47, 040 01 Košice, Slovakia
(Received 27 November 2007; published 12 February 2008)

The ground-state phase diagram of the asymmetric Hubbard model is studied in one and two dimensions by a well-controlled numerical method. The method allows us to calculate directly the probabilities of particular phases in the approximate ground state and thus to specify the stability domains corresponding to phases with the highest probabilities. Depending on the electron filling n and the magnitude of the asymmetry t_f/t_d between the hopping integrals of f and d electrons two different scenarios in formation of ground states are observed. At low electron fillings ($n \leqslant 1/3$) the ground states are always phase segregated in the limit of strong asymmetry ($t_d \gg t_f$). With decreasing asymmetry the system undergoes a transition to the phase-separated state and then to the homogeneous state. For electron fillings $n > 1/3$ and weak Coulomb interactions the ground state is homogeneous for all values of asymmetry, while for intermediate and strong interactions the system exhibits the same sequence of phase transitions as for n small. Moreover, it is shown that the segregated phase is significantly stabilized with increasing electron filling, while the separated phases disappear gradually from the ground-state phase diagrams.

DOI: 10.1103/PhysRevB.77.085110 PACS number(s): 71.27.+a, 75.10.Lp, 71.28.+d, 71.30.+h

I. INTRODUCTION

The asymmetric Hubbard model is one of the simplest models for a description of correlated fermions on the lattice. It has been used in the literature to study a great variety of many-body effects in rare-earth and transition-metal compounds, of which quantum phase transitions, mixed-valence phenomena, charge-density waves, and electronic ferroelectricity are the most common examples.[1–5] In the past few years the asymmetric Hubbard model was also used for a description of ground-state properties of fermionic particles on the optical lattice.[6,7] The model consists of two species of electrons: heavy f electrons and light d electrons. The Hamiltonian of the model is

$$H = -t_d \sum_{\langle ij \rangle} d_i^+ d_j - t_f \sum_{\langle ij \rangle} f_i^+ f_j + U \sum_i f_i^+ f_i d_i^+ d_i, \qquad (1)$$

where $f_i^+(f_i)$ and $d_i^+(d_i)$ are the creation (annihilation) operators of heavy and light electrons at lattice site i.

The first two terms of Eq. (1) are the kinetic energies corresponding to quantum-mechanical hopping of d and f electrons between the nearest neighbor sites i and j with hopping probabilities t_d and t_f, respectively. The third term represents the on-site Coulomb interaction between the d electrons with density $n_d = \frac{1}{L}\Sigma_i d_i^+ d_i$ and the f electrons with density $n_f = \frac{1}{L}\Sigma_i f_i^+ f_i$, where L is the number of lattice sites. The model is called "asymmetric" because the hopping integrals for d and f electrons may be different. Usually, the hopping integral of the d electrons is taken to be the unit of energy ($t_d = 1$) and the f-electron hopping integral is considered in the limit $t_f \ll 1$. This is a reason why the d electrons are called light and the f electrons heavy. The Hamiltonian (1) reduces to the spinless Falicov-Kimball model for $t_f = 0$ and to the usual one-band Hubbard model for $t_f = 1$. Thus the asymmetric Hubbard model can we viewed as a generalized Falicov-Kimball model and also as a generalized one-band Hubbard model.

The first systematic study of ground-state properties of the asymmetric Hubbard model has been performed by Domanski and co-workers using various analytical and numerical techniques.[1,8–10] In the first paper from this series the authors studied the ground-state properties of the one-dimensional asymmetric Hubbard model by their own approximate method that allowed them to treat larger clusters than accessible by exact-diagonalization technique. Their method was based on the sequence of two steps. First, they found the lowest-energy state for every permissible f-electron configuration, similarly as in the pure spinless Falicov-Kimball model ($t_f = 0$). To do this the matrices of rank $\frac{L!}{(L-N_d)!N_d!}$ had to be diagonalized. Second, they took the states thus found as a basis of a new matrix of rank $\frac{L!}{(L-N_f)!N_f!}$ that was subsequently diagonalized. The lowest-energy eigenstate of this matrix was then used to construct the approximate ground state. The main result obtained by the application of this method to the asymmetric Hubbard model was that the motion of the heavy electrons is strongly influenced by the light ones, while the light electrons are almost unaffected by the presence of the heavy ones. The subsequent study[8] of the asymmetric Hubbard model on the one-dimensional ring with two f and two d electrons showed that an effective attraction between two f electrons can be produced by correlation effects for a certain set of the model parameters. The same result, an effective attraction between two heavy electrons mediated by two light electrons leading to the phase segregation, was confirmed also in two dimensions.[10] These studies showed that the phase segregation is owned not only to the Falicov-Kimball model,[11] but persists also at finite t_f. For strong interactions this result was proven rigorously by Ueltschi.[12] The boundary of the phase segregation and/or separation region in the U-t_f plane has been calculated very recently by two different methods. To identify the transition boundary Gu *et al.*[7] used the quantum entanglement between a local part and the rest of the system and the structure factor of charge-density wave for heavy electrons. Away from half-filling, they found that the domain of phase separation is not

confined only to small t_f, but persists up to relative large values of t_f (e.g., $t_f \sim 0.2$ for intermediate Coulomb interactions $U \sim 5$) and with increasing U is further stabilized. The same result has been obtained also by Wang *et al.* using the bosonization method.[5]

In the current paper we study the ground-state phase diagram of the asymmetric Hubbard model by an improved Lyzwa-Domanski scheme[1] discussed above. The advantage of this method is that it can treat much larger clusters than accessible by exact-diagonalization technique and its applicability, unlike the density matrix renormalization group (DMRG)[7] or bosonization[5] method, is not confined only to the one-dimensional case. Moreover, the method allows us to calculate directly the probabilities of particular f-electron configurations and thus to specify the stability domains corresponding to distributions with the highest probabilities.

II. METHOD

Before discussing our approach, it is useful and instructive to summarize the main steps of the numerical algorithm leading to the exact solution of the spinless Falicov-Kimball model on finite clusters. The asymmetric Hubbard model (1) reduces to the spinless Falicov-Kimball model for $t_f=0$. Its Hamiltonian reads

$$H_{FKM} = -t_d \sum_{\langle ij \rangle} d_i^+ d_j + U \sum_i f_i^+ f_i d_i^+ d_i. \tag{2}$$

Since in this version, without f-electron hopping, the f-electron occupation number $f_i^+ f_i$ of each site i commutes with the Hamiltonian (2), the f-electron occupation number is a good quantum number and can be replaced by classical variables $w_i=1$ or 0, according to whether or not the site i is occupied by the localized f electron. Then the Hamiltonian (2) can be written as

$$\mathcal{H}_{\mathcal{FKM}} = \sum_{ij} h_{ij} d_i^+ d_j, \tag{3}$$

where $h_{ij}(w)=-t_d$, if i and j are the nearest neighbor; $h_{ij}(w)=Uw_i$, if $i=j$ and zero otherwise.

Thus for a given f-electron configuration $w=\{w_1, w_2 \ldots w_L\}$ defined on the one-, two-, or three-dimensional lattice, the Hamiltonian (3) is the second-quantized version of the single-particle Hamiltonian and can be directly diagonalized by the following canonical transformation:

$$d_\alpha^+(w) = \sum_i V_{i\alpha}^{(w)} d_i^+, \tag{4}$$

where $V^{(w)}$ is the unitary matrix that diagonalizes $h(w)$. The ground state of $\mathcal{H}_{\mathcal{FKM}}$ is then constructed as follows:

$$|\psi_w^d\rangle = \prod_{\alpha=1}^{N_d} d_\alpha^+(w)|0\rangle \tag{5}$$

and the corresponding ground-state energy is simply given by

$$E_0(w) = \sum_{\alpha=1}^{N_d} \varepsilon_\alpha(w), \tag{6}$$

where $\varepsilon_\alpha(\varepsilon_1 < \varepsilon_2 < \cdots < \varepsilon_L)$ are eigenvalues of the single-particle matrix $h(w)$.

Generalizing this procedure our approach to the full Hamiltonian of the asymmetric Hubbard model (1) can be formulated in the following two points: First, we construct the reduced basis $|\psi_k\rangle$ of H by making the ansatz

$$|\psi_k\rangle = |\psi_k^f\rangle|\psi_k^d\rangle, \tag{7}$$

where $|\psi_k^f\rangle$ is the complete set of eigenstates of the f-electron subsystem $\left(k=1,2,\ldots,\frac{L!}{(L-N_f)!N_f!}\right)$ and $|\psi_k^d\rangle$ is the ground state corresponding to $|\psi_k^f\rangle$ (note that $f_i^+ f_i|\psi_k^f\rangle = w_i^{(k)}|\psi_k^f\rangle$). Second, the reduced basis $|\psi_k\rangle$ is used to calculate the matrix elements $H_{nm}=\langle\psi_n|H|\psi_m\rangle$ of the full Hamiltonian (1). This matrix is then diagonalized and its lowest-energy eigenvalue E_1 yields the upper bound for the ground-state energy of H. The corresponding eigenvector

$$|\psi_G\rangle = \sum_n U_{n,1}|\psi_n\rangle \tag{8}$$

(where U_{nm} is the unitary matrix that diagonalizes H_{nm}) is the approximate ground state and can be used directly to calculate the expectation value of any operator $\langle\hat{A}\rangle=\langle\psi_G|\hat{A}|\psi_G\rangle$. Using expressions (4)–(8) one can show easily that any ground-state expectation value can be written directly in terms of the unitary matrices $V^{(w)}$ that diagonalize the single-particle matrices $h(w)$ corresponding to all possible distributions of f electrons.

To establish connection between our approach and that of Lyzwa and Domanski let us calculate explicitly the matrix elements H_{nm} of the total Hamiltonian of the asymmetric Hubbard model (1). Making use of the fact that the new creation (d_α^+) and annihilation (d_α) operators obey the following commutation relation:

$$d_\alpha(n)d_\beta^+(m) + d_\beta^+(m)d_\alpha(n) = k_{\alpha\beta}(n,m), \tag{9}$$

where the matrix elements $k_{\alpha\beta}$ are given by

$$k_{\alpha\beta}(n,m) = \sum_i V_{i\alpha}^{(n)} V_{i\beta}^{(m)}, \tag{10}$$

the straightforward calculations lead to the following expressions for the diagonal and off-diagonal matrix elements of H:

$$H_{nn} = E_0(n) \tag{11}$$

and

$$H_{nm} = -t_f \langle\psi_n^f| \sum_{\langle ij \rangle} f_i^+ f_j |\psi_m^f\rangle = -(-1)^s t_f \det(k(n,m)), \tag{12}$$

where s is the number of permutations that should be done to transform ψ_m^f on ψ_n^f by $f_i^+ f_j$. As discussed bellow the Lyzwa-Domanski approach can be recovered directly from Eq. (12) by putting $\det(k)=1$, however, generally $\det(k) \neq 1$.

To test our method we have first calculated the ground-state energy of the asymmetric Hubbard model for various

TABLE I. The ground-state energy of the one-dimensional asymmetric Hubbard model calculated for three different values of Coulomb interaction U on finite clusters of $L=6$ and $L=10$ sites at $t_f=1$ and $n_f=n_d=1/2$. Different columns correspond to exact results (Exact), Lyzwa-Domanski approach (Approx. I), and our approach (Approx. II).

	$L=6$			$L=10$		
U	Exact	Approx. I	Approx. II	Exact	Approx. I	Approx. II
0.1	−1.30850	−1.30868	−1.30830	−1.26960	−1.26978	−1.26934
1.0	−1.10019	−1.11770	−1.08064	−1.06144	−1.08013	−1.03697
10	−0.27739	−0.73823	−0.20421	−0.27037	−0.71753	−0.19908

model parameters (t_f, U) on small one-dimensional clusters where exact results are also accessible. In Tables I and II we present the exact and approximate ground-state energies obtained for the finite clusters of $L=6$ and 10 sites, two representative values of t_f $(t_f=0.1,1)$, and three representative values of U $(U=0.1,1,10)$. For a comparison we have included in Table I also results obtained by Lyzwa and Domanski[1] and we have verified numerically that these results can be recovered exactly by our method simply putting $\det(k)=1$ in Eq. (12). Comparing these results one can see that both approaches work very well in the weak-coupling limit $(U \leq 1)$, while in the opposite limit $(U \gg 1)$ our method yields a considerable better estimation of the ground-state energy than that of Lyzwa and Domanski. Figure 1 demonstrates that this trend holds also for smaller values of t_f. Moreover, as one can expect intuitively, the accordance between our results and the exact ones considerably improves with decreasing t_f and for a sufficiently strong asymmetry $(t_f \sim 0.2)$ a nice accordance of results is observed over the whole interval of Coulomb interactions (see also Table II).

To verify the ability of our method to describe the main characteristics of the exact ground state we have also calculated the f-electron pair correlation function $L(x)$ defined by[1]

$$L(x) = \frac{1}{L}\sum_j \langle f_j^+ f_j f_{j+x}^+ f_{j+x} \rangle. \tag{13}$$

The results of numerical computations are summarized in Fig. 2. It is seen that a nice accordance with exact behaviors is obtained in the weak- $(U=1)$ as well as strong- $(U=10)$ coupling limits for both small $(t_f \leq 0.2)$ and intermediate $(t_f \sim 0.4)$ values of f-electron hopping integrals.

III. PHASE DIAGRAMS

A. One-dimensional case

One of the greatest advantages of the method discussed above is that it allows us to calculate directly the probability of any f-electron configuration in the approximate ground state. We used this fact to construct the phase diagrams of the asymmetric Hubbard model in the t_f-U plane for various sizes of clusters and electron fillings. The phases presented in the phase diagrams are those corresponding to f-electron distributions with the highest probabilities for given values of t_f and U.

The typical examples of ground-state phase diagrams of the asymmetric Hubbard model are displayed in Fig. 3 for $L=24$ and four representative values of f-electron filling n_f (note that $n_d=n_f=n/2$). A general feature which can be noticed in these pictures is that the basic structure of the phase diagrams is formed by only two main types of the f-electron configurations and, namely, the most homogeneous distributions (MHDs) (the f electrons are distributed homogeneously over the whole lattice) and the phase-separated configurations (the f electrons occupy only one part of the lattice while the remaining one is empty). As discussed below, between the phase-separated and phase-segregated configurations the special role is played by the phase-segregated configurations (all f electrons clump together) and therefore they are considered here as the independent group. In the language of an effective interaction between the f electrons, the most homogeneous configurations correspond to an effective repulsion and the phase-separated and/or -segregated configurations to an effective attraction between the f electrons. From this point of view, it is very interesting that in the pure electronic system (with only the on-site Coulomb repulsion between the light and heavy electrons) an effective attraction

TABLE II. The ground-state energy of the one-dimensional asymmetric Hubbard model calculated for three different values of Coulomb interaction U on finite clusters of $L=6,10$ and $L=14$ sites at $t_f=0.1$ and $n_f=n_d=1/2$. Different columns correspond to exact results (Exact) and our approach (Approx. II).

	$L=6$		$L=10$		$L=14$	
U	Exact	Approx. II	Exact	Approx. II	Exact	Approx. II
0.1	−0.70864	−0.70864	−0.68725	−0.68725	−0.68152	−0.68151
1.0	−0.51544	−0.51507	−0.49546	−0.49495	−0.49047	−0.48986
10	−0.10056	−0.09961	−0.10015	−0.09925	−0.10018	−0.09923

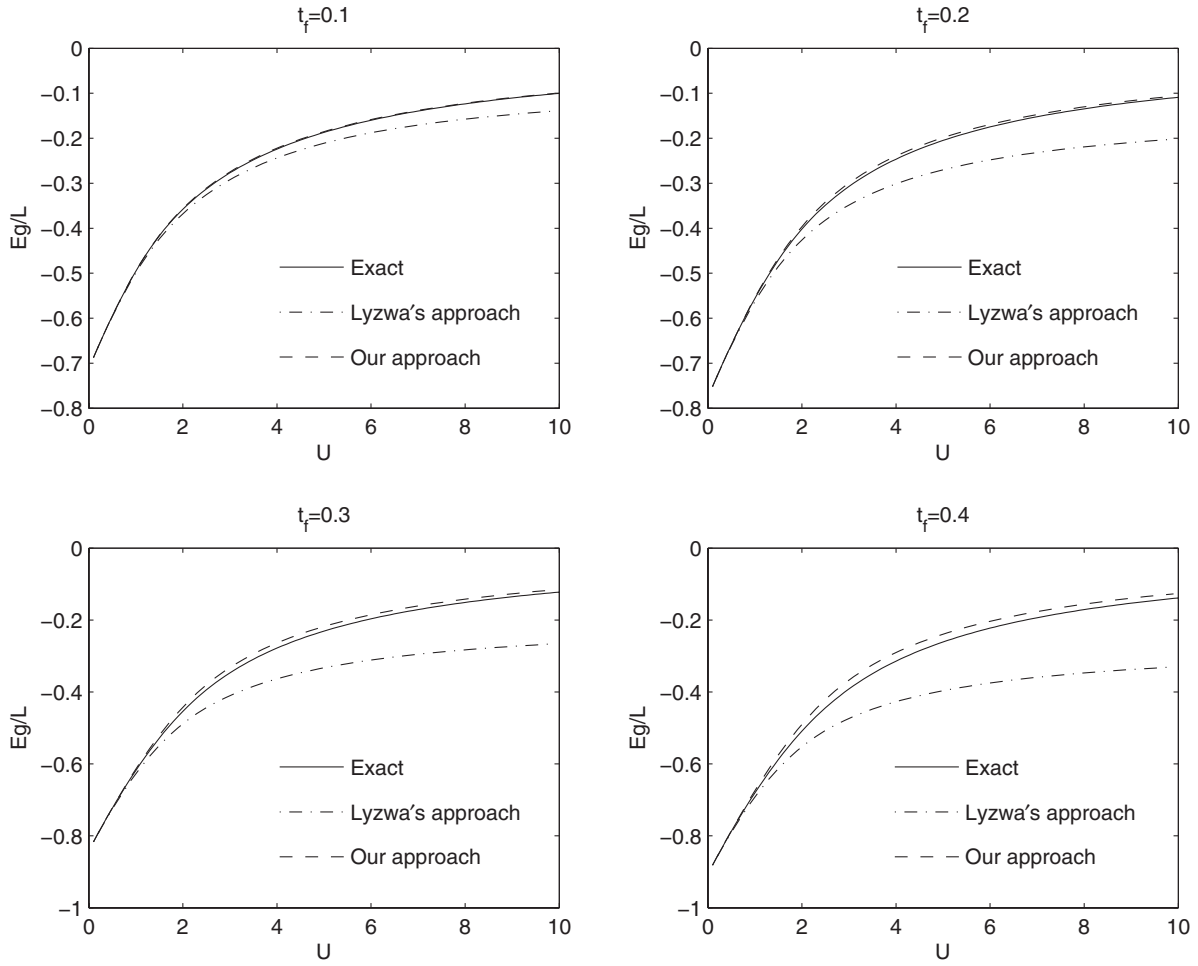

FIG. 1. The ground-state energy of the asymmetric Hubbard model as a function of U calculated for four different values of t_f and $L=10$. Different lines correspond to exact results (solid line), our approach (dashed line), and Lyzwa-Domanski approach (dash-dotted line). The half-filled band case ($n_f=n_d=1/2$).

between the f electrons is produced, even for t_f away from the Falicov-Kimball limit $t_f=0$. Indeed, our results show that the phase boundary $t_f^c(U)$ between the most homogeneous and phase-separated and/or -segregated regions increases rapidly with increasing U and reaches the intermediate values $t_f^c(U)\sim 0.25$ already for intermediate Coulomb interactions. In the weak-coupling and low density limits, the phase boundary scales like $t_f^c(U)\sim U^2$, while at higher electron fillings ($n_f=1/4$ and $n_f=1/3$) the phase-separated and/or -segregated distributions are stabilized above some critical value of Coulomb interaction U ($U\sim 0.5$ for $n_f=1/4$ and $U\sim 2.2$ for $n_f=1/3$). In these limiting cases our results reproduce the analytical and numerical results obtained recently by bosonization[5] and exact-diagonalization and/or DMRG methods.[7] Comparing our results with the exact-diagonalization and/or DMRG results[7] ($n_f=1/4$) one can see that these results agree very well in spite of the fact that fully different approaches have been used to identify the phase-separated region.

The advantage of our method is that it also allows us to identify the internal structure of the phase diagrams and thereby to study how this structure changes by varying the model parameters. Figure 3 shows that the phase diagrams of the asymmetric Hubbard model (strictly said the phase-separated domains) have a rich internal structure that exhibits some general trends. First, the phase-separated region starts with the phase-segregated distribution. Small exceptions are found only for $n_f=1/4$ and $n_f=1/3$, where also some other phases are observed for $t_f\to 0$, but their stability regions are very limited. Second, the segregated cluster of length N_f splits into two or more smaller clusters with increasing t_f. Third, the segregated configuration is stabilized with increasing electron filling, while the separated phases disappear from the phase diagrams.

Although the cluster used in our numerical calculations is relatively large ($L=24$) to exclude completely the finite size effects the same calculations have been performed on several different clusters for each selected value of electron filling. We have found that the fundamental characteristics of the phase diagrams discussed above and, namely, the phase boundary between the phase-separated and most homogeneous phase, the phase boundary of segregated phase, and the critical value of Coulomb interactions at which the phase separation starts for large f-electron fillings are almost independent of L. This is clearly demonstrated in Fig. 4 where the boundary of phase separation is plotted for two different values of n_f ($n_f=1/4$ and $n_f=1/3$). This analysis indicates

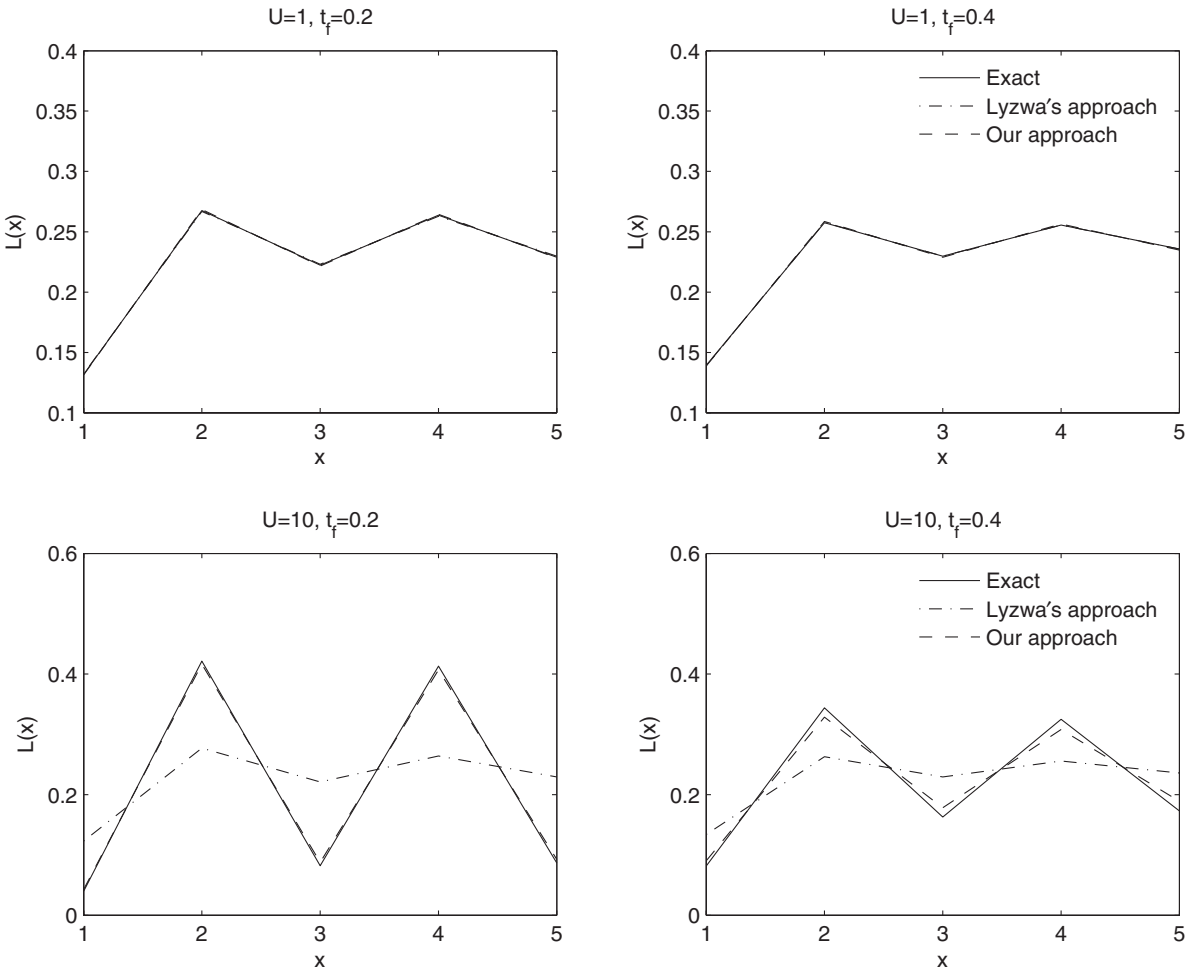

FIG. 2. The f-electron pair correlation function $L(x)$ of the asymmetric Hubbard model calculated for two different values of U and t_f at $L=10$. Different lines correspond to exact results (solid line), our approach (dashed line), and Lyzwa-Domanski approach (dash-dotted line). The half-filled band case ($n_f=n_d=1/2$).

that our one-dimensional results can be extrapolated satisfactorily to the thermodynamic limit ($L\rightarrow\infty$).

B. Two-dimensional case

Since the phenomenon of phase separation is one of the most interesting problems in the condensed matter physics we extend our calculations also on the two-dimensional case. As discussed above such an extension is possible due to the fact that instead the full Hilbert space we work only with the reduced basis and corresponding reduced matrices of rank $\frac{L!}{(L-N_f)!N_f!}$. This allows us to study the two-dimensional clusters up to 6×6 sites that are far away beyond the reach of present day computers within the exact-diagonalization calculations. The results of our numerical calculations obtained for two different values of electron fillings are summarized in Fig. 5 in the form of t_f-U phase diagrams together with the complete list of f-electron configurations with the highest probabilities. It is seen that all main features of the one-dimensional phase diagrams hold in two dimensions, too. For small values of f-electron hopping the system is phase segregated and/or separated, while increasing t_f stabilizes the homogeneous distribution of f electrons. In accordance with the one-dimensional case we have found that the phase boundary $t_f^c(U)$ between the homogeneous and phase-separated region scales like U^2 for weak interactions, and that the region of phase segregation and/or separation increases rapidly with increasing n_f.

In summary, we have presented an improved numerical scheme for calculating ground-state properties of the asymmetric Hubbard model. The advantage of this method is that it can treat much larger clusters than accessible by exact-diagonalization technique and its applicability, unlike the DMRG or bosonization method, is not confined only to the one-dimensional case. Moreover, the method allows us to calculate directly the probabilities of particular f-electron configurations and thus to specify the stability domains corresponding to distributions with the highest probabilities. We have used this fact to construct the ground-state phase diagrams of the asymmetric Hubbard model in one and two dimensions for a wide range of model parameters. We have found that at low electron fillings ($n\leq 1/3$) the ground states are always phase segregated for a strong asymmetry between the hopping integral of d and f electrons ($t_d \gg t_f$). With decreasing asymmetry the system undergoes a transition to the

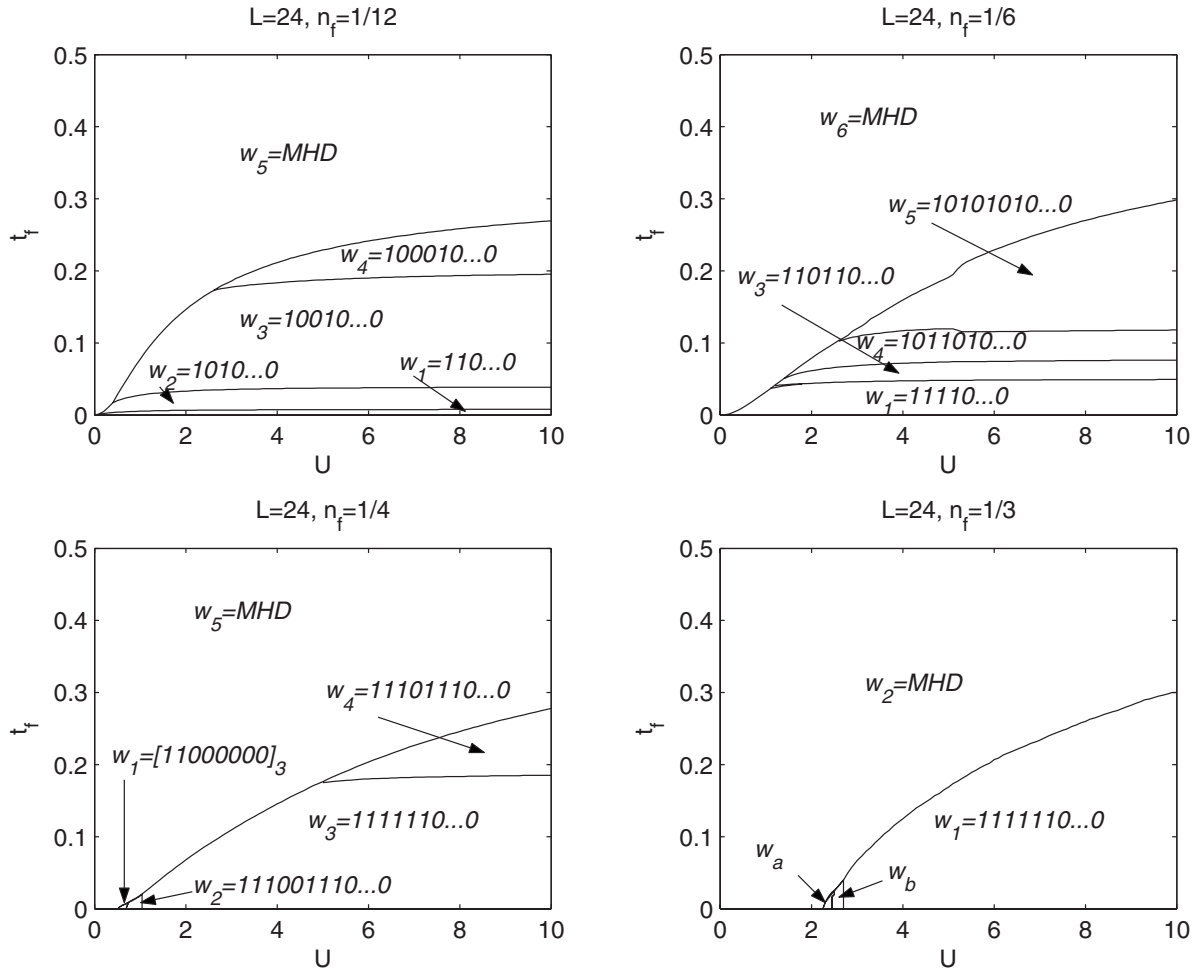

FIG. 3. The ground-state phase diagram of the one-dimensional asymmetric Hubbard model calculated for several f-electron densities on finite cluster of $L=24$ sites. Depicted domains represent the stability regions of the f-electron configurations with the highest probabilities in the approximate ground state. Two small domains w_a and w_b (for $n_f=1/3$) consist of several subdomains: $w_a^1=[110000]_4$, $w_a^2=[110011000000]_2$; $w_b^1=[1100]_4 00000000$, $w_b^2=111001100111000000000000$, $w_b^3=[111100]_2 000000000000$, where the lower index denotes the number of repetitions of the block $[\cdots]$.

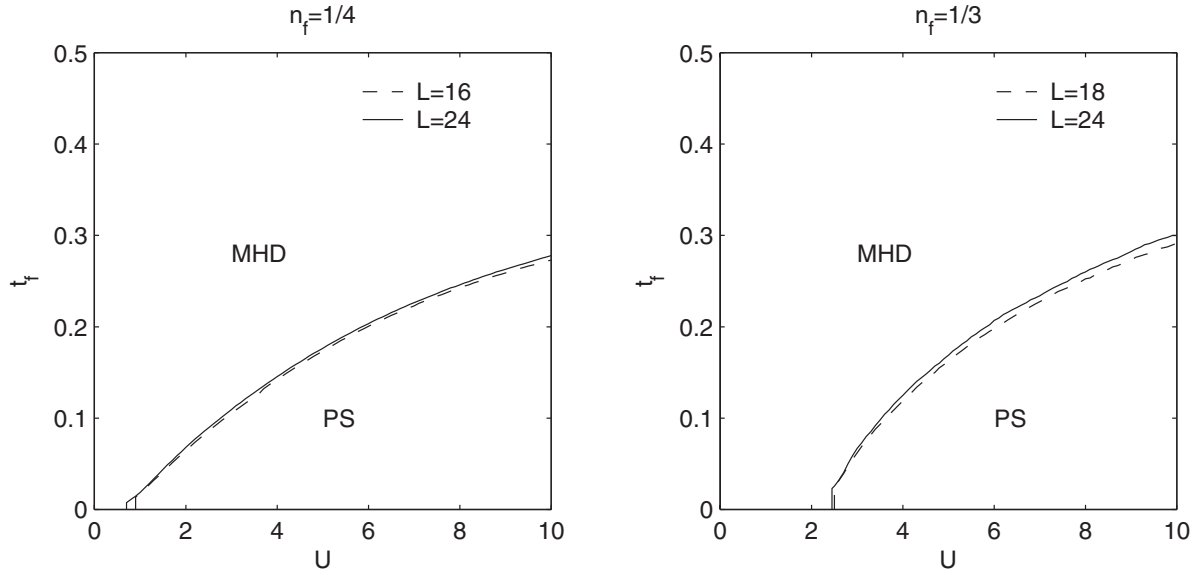

FIG. 4. The phase boundary between the most homogeneous distribution (MHD) and phase-separated (PS) domain as a function of U. Comparison of our numerical results obtained on different finite clusters for $n_f=1/4$ and $n_f=1/3$.

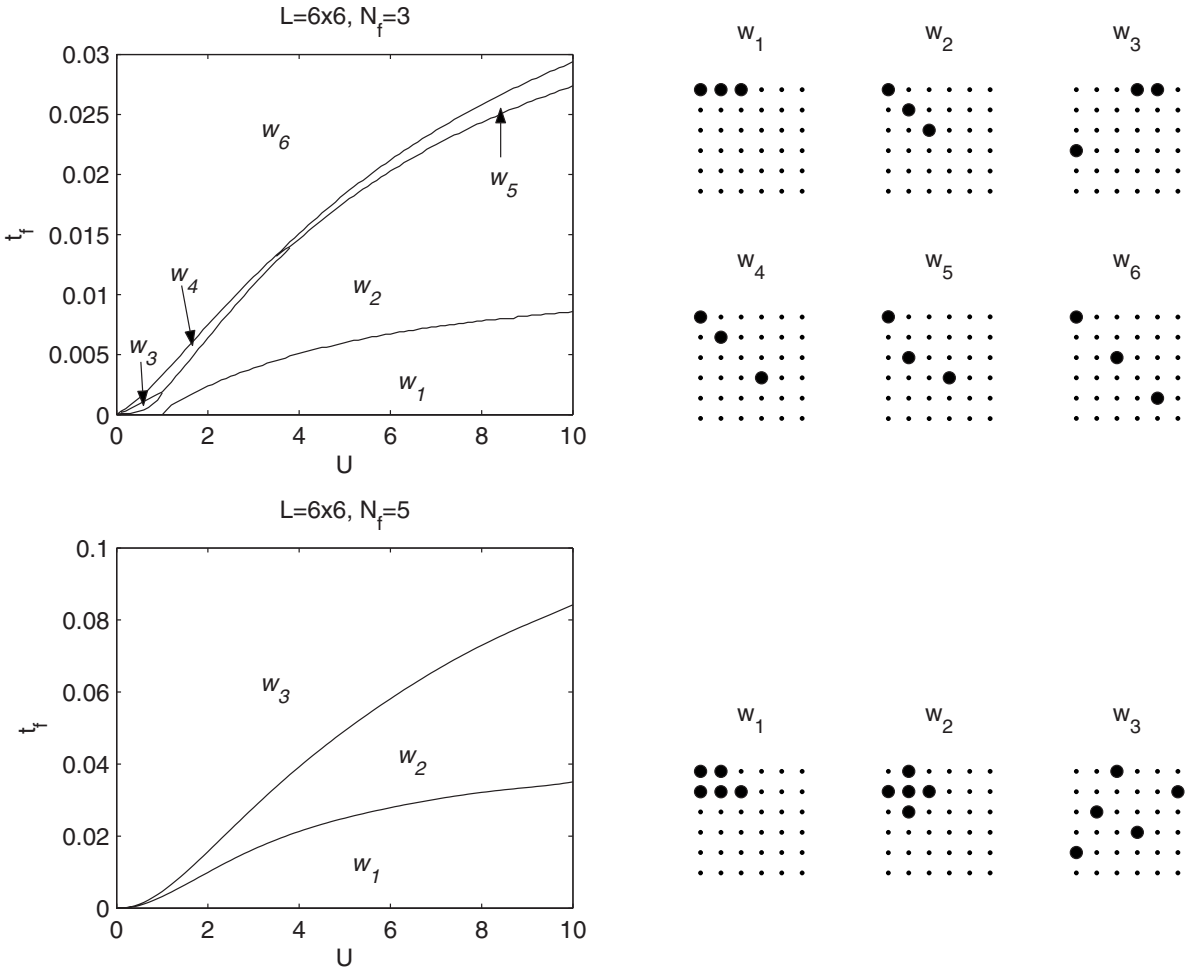

FIG. 5. The ground-state phase diagram of the two-dimensional asymmetric Hubbard model calculated for two f-electron densities on finite cluster of $L=36$ sites with the complete list of f-electron configurations with the highest probabilities.

phase-separated state and then to the homogeneous state. For electron fillings $n>1/3$ and weak Coulomb interactions the ground state (in one dimension) is homogeneous for all values of asymmetry, while for intermediate and strong interactions the system exhibits the same sequence of phase transitions as for n small.

ACKNOWLEDGMENTS

This work was supported by the Slovak Grant Agency for Science under Grant No. 2/7057/27 and the Slovak APVV Grant Agency under Grant No. LPP-0047-06. I would also like to acknowledge H. Čenčariková for technical help during the preparation of the manuscript.

[1] R. Lyzwa and Z. Domanski, Phys. Rev. B **50**, 11381 (1994).

[2] C. D. Batista, Phys. Rev. Lett. **89**, 166403 (2002); C. D. Batista, J. E. Gubernatis, J. Bonca, and H. Q. Lin, *ibid.* **92**, 187601 (2004).

[3] W. G. Yin, W. N. Mei, Ch. G. Duan, H. Q. Lin, and J. R. Hardy, Phys. Rev. B **68**, 075111 (2003).

[4] A. M. C. Souza and C. A. Macedo, Physica B **384**, 196 (2006).

[5] Z. G. Wang, Y. G. Chen, and S. J. Gu, Phys. Rev. B **75**, 165111 (2007).

[6] J. Silva-Valencia, R. Franco, and M. S. Figueira, Physica B **398**, 427 (2007).

[7] S. J. Gu, R. Fan, and H. Q. Lin, Phys. Rev. B **76**, 125107 (2007).

[8] Z. Domanski, R. Lyzwa, and P. Erdos, J. Magn. Magn. Mater. **140**, 1205 (1995).

[9] G. Fath, Z. Domanski, and R. Lemanski, Phys. Rev. B **52**, 13910 (1995).

[10] Z. Domanski, R. Lemanski, and G. Fath, J. Phys.: Condens. Matter **8**, L261 (1996).

[11] J. K. Freericks, E. H. Lieb, and D. Ueltschi, Phys. Rev. Lett. **88**, 106401 (2002).

[12] D. Ueltschi, J. Stat. Phys. **116**, 681 (2004).